Global warming is increasing the discrepancy between the thermal (potential) and green (actual) seasons of temperate trees

Authors: Yongshuo H. Fu[1*], Xiaojun Geng [1,2], Hao Wu[3], Shouzhi Chen[1], Fanghua Hao[3*], Xuan Zhang[1], Zhaofei Wu[1], Jing Zhang[1], Jing Tang[4,5,6], Yann Vitasse[7], Constantin M. Zohner[8], Ivan Janssens[9], Nils Chr. Stenseth[10,11], Josep Peñuelas[12]

Affiliations

[1] College of Water Sciences, Beijing Normal University, Beijing 100875, China.

[2] General Institute of Water Resources and Hydropower Planning and Design (GIWP), Ministry of Water Resources, Beijing, China.

[3] College of Urban and Environmental Sciences, Central China Normal University, Wuhan 430079, China

[4] Department of Physical Geography and Ecosystem Science, Lund University, Sölvegatan 12, SE-223 62, Lund, Sweden.

[5] Terrestrial Ecology Section, Department of Biology, University of Copenhagen, DK-2100, Copenhagen, Denmark.

[6] Center for Permafrost (CENPERM), University of Copenhagen, DK-1350, Copenhagen, Denmark.

[7] Swiss Federal Institute for Forest, Snow and Landscape Research (WSL), Birmensdorf, Switzerland

[8] Institute of Integrative Biology, ETH Zurich (Swiss Federal Institute of Technology), Zurich, Switzerland

[9] Plants and Ecosystems, Department of Biology, University of Antwerp, Antwerp, Belgium.

[10] CREAF, Cerdanyola del Vallès, Barcelona 08193, Catalonia, Spain.

[11] CSIC, Global Ecology Unit CREAF-CSIC-UAB, Bellaterra, Barcelona 08193, Catalonia, Spain.

[12] Centre for Ecological and Evolutionary Synthesis (CEES), Department of Biosciences, University of Oslo, N-0316 Oslo, Norway

Corresponding author: Yongshuo H. Fu & Fanghua Hao
Phone: +86-58802736
Email: yfu@bnu.edu.cn; fhhao@ccnu.edu.cn

Competing interest statement: The authors declare no competing interests.

Key words: Climatic warming, thermal season, green season, spring leaf-out, autumnal foliar senescence

Abstract

Over the past decades, global warming has led to a lengthening of the time window during which temperatures remain favorable for carbon assimilation and tree growth, resulting in a lengthening of the green season. The extent to which forest green seasons have tracked the lengthening of this favorable period under climate warming, however, has not been quantified to date. Here, we used remote sensing data and long-term ground observations of leaf-out and coloration for six dominant species of European trees at 1773 sites, for a total of 6060 species–site combinations, during 1980–2016 and found that actual green season extensions (GS: 3.1 ± 0.1 day decade−1) lag four times behind extensions of the potential thermal season (TS: 12.6 ± 0.1 day decade−1). Similar but less pronounced differences were obtained using satellitederived vegetation phenology observations, that is, a lengthening of 4.4 ± 0.13 and 7.5 ± 0.13 day decade−1 for GS and TS, respectively. This difference was mainly driven by the larger advance in the onset of the thermal season compared to the actual advance of leaf-out dates (spring mismatch: 7.2 ± 0.1 day decade−1), but to a less extent caused by a phenological mismatch between GS and TS in autumn (2.4 ± 0.1 day decade−1). Our results showed that forest trees do not linearly track the new thermal window extension, indicating more complex interactions between winter and spring temperatures and photoperiod and a justification of demonstrating that using more sophisticated models that include the influence of chilling and photoperiod is needed to accurately predict spring phenological changes under warmer climate. They urge caution if such mechanisms are omitted to predict, for example, how vegetative health and growth, species distribution and crop yields will change in the future.

KEYWORDS

autumnal foliar senescence, climatic warming, green season, spring leaf-out, thermal season

Introduction

The last three decades were the warmest in the last 800 years (Legg, 2021), leading to a lengthening of the time window during which temperatures remain favorable for tree growth in the extra-tropical regions. Thermal accumulation during the time window (potential thermal season, TS) plays a key role in the forest health (Hicke et al., 2012; Trumbore, Brando, & Hartmann, 2015), crop yields (Ketring & Wheless, 1989; Zimmermann et al., 2017), vegetation growth and the geographic distribution of species (Chuine, 2010; Fang & Lechowicz, 2006). Recent warming has extended the latitudinal and altitudinal distributions of tree species (Beck & Goetz, 2011; Chuine, 2010), albeit at a slower rate than the shift of their thermal niche due to demographic processes and interspecific competition (Huang et al., 2017; Scherrer, Vitasse, Guisan, Wohlgemuth, & Lischke, 2020; Vitasse et al., 2021). Phenology is highly sensitive to temperature and plays a key role in driving the distributions of plant species (Chuine, 2010; Körner et al., 2016). Global warming has also led to a lengthening of the growing season for plants at mid- to high latitudes of the Northern Hemisphere, which in turn has affected the carbon (a longer growing season increased the carbon uptake especially in autumn) and water cycles (a longer growth season reduced the runoffs and a scale different between phenology and water flux) of terrestrial ecosystems and thereby the climatic system (Chen et al., 2022; Cleland, Chuine, Menzel, Mooney, & Schwartz, 2007; Keenan & Richardson, 2015; Kim et al., 2018; Peñuelas, Rutishauser, & Filella, 2009; Piao et al., 2019). The extent to which vegetation green seasons have tracked the lengthening of this favorable period during this abrupt warming, however, is unclear.

It's therefore essential understanding how trees' phenological cycles adapt to a rapidly warming climate, which will ultimately improve projections of future changes in the forest system and the multiple ecosystem services it provides.

Climatic warming is currently extending the vegetation growing season in the extra-tropical regions by advancing spring leaf-out and delaying autumnal foliar senescence (Chmielewski & Rötzer, 2001; Q. Liu et al., 2018; Piao et al., 2019; Zhu et al., 2012). Many studies have documented these responses of vegetative activity to a changing environment (Friend et al., 2014; Peaucelle et al., 2019; Wu et al., 2015), but increasing evidence also suggests that the sensitivity of phenology to climatic warming is decreasing. For example, the spring leaf phenology of six common species of European deciduous trees has become less sensitive to warming in recent decades (Y. H. Fu, Zhao, et al., 2015). Accordingly, the heat unit required for leaf-out in temperate European trees has increased by 50% with climatic warming (Y. H. Fu, Piao, et al., 2015). Similarly, even though the timing of foliar senescence in autumn has been reported to be less responsive to temperature than the timing of spring leaf-out, the heat unit required for autumnal phenology has also increased in recent decades (Menzel et al., 2020; Zani, Crowther, Mo, Renner, & Zohner, 2020). These findings indicate that climatic warming-induced increases in TS do not necessarily translate to a linear extension of the actual vegetation green season extensions (GS). In other words, the heat unit requirement of plants may change under warmer environments, introducing large uncertainties and possibly errors in the predictions of future vegetation

productivity and species distributions when thermal sums are used (Chuine, 2010; Chuine & Beaubien, 2001; Chuine et al., 2016; Keenan et al., 2014; Park et al., 2016). Investigating the temporal overlap and potential lag between vegetation phenology and favorable climatic conditions is critical to improving our understanding of the responses of vegetation to the ongoing climate change (Linderholm, 2006; Piao et al., 2020).

In this study, we examined whether the GS, defined as the period from leaf-out in spring to foliar senescence in autumn, has been tracking the ongoing lengthening of the TS, classically defined as the period from the first day of the year when daily air temperatures were >5 °C for more than five consecutive days to the last day of the year when daily air temperatures were <5 °C for more than five consecutive days. We used long-term phenological observations of six widely distributed tree species at 1773 sites in central Europe and a satellite-derived phenology dataset between 1980-2016 (Site locations and distribution of each species detailed in Fig. S1) to address the following questions: (1) to what extent have GS and TS changed over 1980-2016 and (2) has climatic warming uncoupled TS and GS, and if so, what are the underlying mechanisms?

Results and discussion

Mean annual temperature in the study area increased at an average rate of 0.39 ± 0.11 ℃ decade^{-1} during 1980-2016 (Fig. S2). Based on the in situ phenology observations, both GS and TS lengthened during this period, but the lengthening of TS was four times greater than the one GS extensions (+12.6 ± 0.1 d decade^{-1} versus +3.1 ± 0.1 d decade^{-}

[1], respectively), leading to an increase of 9.5 ± 0.1 d decade^{-1} in the mismatch between TS and GS (δGS, Fig. 1a). Both TS and GS tended to extend across 73.5% of the 6060 species-site combinations, with ~50% of these extensions significant at $P \leq 0.05$ (Fig. 1b). Similar results were found for each of the six studied species, with δGS ranging from 7.9 to 11.1 d decade^{-1} across species (Figs. 1c and S3). To compare with the *in situ* species-based results, we also explored the δGS across the study region using gridded climate data and satellite-based phenological observations (see Materials and methods), and we found similar patterns, with GS and TS extending by +4.4 ± 0.13 d decade^{-1} and +7.5 ± 0.13 d decade^{-1}, respectively (Fig. 2). Nevertheless, the difference between GS and TS was smaller for the remote sensing results than for the *in situ* results, which can likely be attributed to differences in species composition (satellite-based phenology dates only reflect the mean phenological dates across the species) and to the uncertainty in the satellite-derived phenological dates, e.g. pixel mixing effect. And we used six species because they are most widely distributed tree species in Europe, but we are not sure whether they are dominant across all regions in the study area, which indeed may also partially explain the results difference between the in situ and remote-sensing based results.

To test the sensitivity of the GS estimation to the choice of the temperature threshold used to estimate TS, we estimated the δGS using temperature thresholds from 1℃ to 10℃ with one degree steps. Interestingly, we found that the temporal change in the difference between TS and GS (δGS) was largest at a TS threshold of 5℃, which is the most common temperature threshold used in previous studies. These new results justify

the methods previously used and highlight that the selection of the temperature threshold largely affects the inferred temporal trends in TS (Figs. S4 and S5).

Based on the *in situ* phenology observations, both the onset of the green season and the thermal (potential) season were advanced substantially at speed of -3.5 ± 0.1 d decade^{-1} and -10.7 ± 0.1 d decade^{-1}, respectively, leading to an increase of 7.2 ± 0.1 d decade^{-1} in the mismatch between the start of thermal and green season (δSOS, Fig. 3a). Based on the results of Spring Warming model, Sequential model and Parallel model, we found that larger difference between the trend of predicted SOS and TSOS, and this is mainly because we used the vegetation phenology dates (VSOS) to parameterize these models (see Materials and methods and Fig. S6). For the end of the green or thermal season, the temporal changes of the end of green season and the end of thermal season differed in both magnitude and direction. The end of season thermal was delayed by 2.0 ± 0.04 d decade^{-1}, and the end of green season advanced at an average rate of -0.3 ± 0.1 d decade^{-1}, causing an increasing mismatch between the end of thermal and green season (δEOS) of 2.4 ± 0.1 d decade^{-1}. Note that, the leaf coloration (only part of an autumnal hardening syndrome of the entire tree, driven by its genome and executed by hormones) may be large uncertainty to present the leaf senescence. Recent study has reported that the solar-induced chlorophyll fluorescence (SIF) value closely relates to the growth stage, and then may provide an alternative method to extract the autumn phenology (Jeong, 2020; Zhang et al., 2022). δEOS was smaller than δSOS (Fig. 3b) which implies that the increasing difference between TS and GS is mainly due to the

large mismatch in spring rather than autumn. Further quantification of the relative contribution of spring and autumn phenology dates to the overall changes in GS and TS (see Materials and methods) confirmed that δSOS contributed more than δEOS to the increasing mismatch between GS and TS (δGS) in 70% of the 6060 species-site combinations (Fig. S7). These results were similar across all six species (Figs. 3c and S7). To account for species and site effects, we applied a mixed-effects model, including both species and sites as random effects and obtained very similar results as before (See Table S1).

In a next step, we explored the spatial variation in δGS, δSOS and δEOS, which showed that δSOS increases with latitude, whereas δEOS decreases with latitude, resulting in a constant δGS across latitude for all species and sites (ANCOVA, $F = 4.186$, $P < 0.001$; Fig. 4). While at lower latitudes, δSOS and δEOS were similar (increasing mismatch of ~5 d decade^{-1}), toward higher latitudes, δSOS increased significantly (0.54 ± 0.13 d decade^{-1}·°N^{-1}, $P < 0.01$), whereas δEOS decreased significantly (-0.48 ± 0.12 d decade^{-1} °N^{-1}, $P < 0.01$). At higher latitudes, δGS was mainly driven by δSOS, while at lower latitudes it was mainly driven by δEOS (Fig. S8). The latitudinal distribution of the study species is uneven (Fig. S1), and we accounted for this by excluding *Betula pubescens* and *Tilia cordata*, which resulted in very similar results (Fig. S9), suggesting that the species distribution did not drive the latitudinal patterns.

That TS has been extending more than GS implies an increasing mismatch between the thermal season during which trees could be active (favorable conditions) and the

vegetation green season during which trees are actually active. This increasing mismatch might be the result of an acclimatized response to a warmer environment (Hoffmann & Sgrò, 2011; Mora et al., 2015), whereby plants compromise between maximize their season length requirements and minimize their potential exposure to frost in spring and autumn (Augspurger, 2013; Y. H. Fu et al., 2019; Körner et al., 2016; Vitasse et al., 2019) .

Interestingly, the increasing mismatch between TS and GS was mainly due to δSOS rather than δEOS, suggesting that the spring phenology of tree species did not linearly track the warming trend. We propose that the difference between δSOS and δEOS can mainly be attributed to seasonal differences in the amplitudes of warming and the phenological responses between spring and autumn. A higher rate of warming in spring than autumn (Legg, 2021; Renner & Zohner, 2018), and a lower sensitivity of spring than autumnal phenology to temperature, may together have led to a larger δSOS than δEOS. This increasing discrepancy may affect ecosystem functioning, e.g., by lowering frost damage risk due to thermal adaptation, impacting the synchronization between insects and their food plants (Maino, Kong, Hoffmann, Barton, & Kearney, 2016), and increasing the risk of pest damage (Hicke et al., 2012; Trumbore et al., 2015), which subsequently might induce a short-term slump in forest productivity or niche changes (Heberling, McDonough MacKenzie, Fridley, Kalisz, & Primack, 2019; Kellermann & van Riper, 2015; Q. Liu et al., 2018).

To test this, we analyzed the trends in seasonal temperature and indeed found different warming trends among seasons (spring > winter > autumn, Fig. 5a), explaining the larger changes in thermal start than end of the season. We also estimated the partial correlation between the dates of vegetative phenology and preseason temperature (see Materials and methods). The mean partial correlation coefficient between the start of green season and preseason temperature across all sites and species (-0.62 ± 0.19, 89% being significant) was significantly larger than that of the end of green season (+0.22 ± 0.33, with only 30% significant) (Fig. 5b), suggesting that spring phenology is more controlled by temperature than autumn phenology, since autumnal leaf senescence is a precautional process which proceeds before temperature getting cold. Previous studies have reported a positive correlation between spring and autumn phenology (Y. S. Fu et al., 2014; Keenan & Richardson, 2015), which may offset the autumn temperature effect on autumn phenology, and partially constrain delays in the end of green season. As a result, this may likely reduce the overall difference between TS and GS. We further estimated the apparent sensitivities of spring and autumn phenology to temperature (see Materials and methods) and found that the start of green season advanced by -4.8 ± 1.9 d for each degree Celsius increase in spring temperature, whereas the end of green season was delayed by only 1.9 ± 7.1 d $°C^{-1}$ (Fig. 5c), matching our expectations. These results indicate that both the faster warming in spring and the higher, rather than lower, sensitivity of spring phenology to temperature have contributed to the larger shift (advance) in the start of green season compared to the shift (delay) in the end of green season (which is mainly controlled by photoperiod and temperature fluctuates).

The sensitivity of spring phenology to temperature has been reported to decrease with climatic warming, likely due to progressively insufficient chilling to fully break winter dormancy or photoperiodic constraints slowing down bud development (Y. H. Fu et al., 2019; Y. H. Fu, Zhao, et al., 2015; Garonna, de Jong, & Schaepman, 2016; Prevéy et al., 2017). In line with this, we found that the chilling accumulation for the start of green season has decreased significantly by -3.2 ± 3.2 d decade^{-1} (Fig. 5d), which might lead to reduced temperature sensitivity and thus contribute to the increase in δSOS over the study period.

As mentioned above, the magnitude of warming was much smaller in autumn than in spring (Fig. 5a), and, accordingly, the end of thermal season currently occurs only slightly later than in the past. These findings, however, cannot account for the slight advances in the end of green season over recent decades and instead suggest that factors other than autumnal temperature have played a role (Y. H. Fu et al., 2019; Zani et al., 2020). For example, previous studies have found that changes in spring leaf-out affect the dates of autumnal foliar senescence (Y. S. Fu et al., 2014; Keenan & Richardson, 2015), whereby an earlier start of the season translates to advances in the end of the season, offsetting (at least partly) the retarding effect of a warming autumn. Similarly, it was found that the dates of foliar senescence advanced with increased vegetative growth due to an earlier spring phenology, increasing growing-season temperature and/or increasing atmospheric CO_2 concentrations (Asshoff, Zotz, & Körner, 2006;

Zani et al., 2020). Increased cumulative water deficits from either warming-induced enhanced evapotranspiration or from decreased precipitation could also potentially advance foliar senescence (Li et al., 2021). Indeed, we found that seasonal precipitation over the study period (1980-2016) tended to decrease in all seasons, i.e. spring (-9.9 mm decade^{-1}), summer (-9.3 mm decade^{-1}), autumn (-3.1 mm decade^{-1}) and winter (-7.9 mm decade^{-1}), and especially at higher latitudes (Figs. S10 and 5e), which is consistent with previous studies (J. Wang, Liu, Ciais, & Peñuelas, 2022). We took the mean multi-year precipitation of 600 mm as the dividing line to divide the sites into areas may with water deficit and areas with sufficient water. We found that among sites with mean multi-year precipitation of less than 600mm, the δGS at sites with decreased precipitation were larger than those with increased precipitation. However, the difference is not obvious in the sites with mean multi-year precipitation greater than 600mm. (Fig. S11)

The spatial patterns of δSOS and δEOS were of opposite direction, i.e., δSOS increased and δEOS decreased toward higher latitudes, which may be due to spatial variations in warming trends and environmental constraints. The larger difference between advances in the start of thermal and green season (δSOS) at higher latitudes may have been caused by the stronger warming trends that have occurred over recent decades at higher latitudes (larger advance in TSOS, Fig. S12), whereas advances in the start of green season show no clear latitudinal pattern. Indeed, the spatial differences in the temporal trends in the start of green season were small (Fig. S13), indicating that other

environmental constraints, such as photoperiod and local microclimate, may have buffered against warming-induced advances in leaf-out (Y. H. Fu et al., 2019; Tang et al., 2016). To test whether the stronger buffering at higher latitudes could be due to the effect of photoperiod, we used the standard deviation of phenological dates as an indirect measure of the effect of photoperiod following previous studies (Geng et al., 2022; Zohner, Benito, Svenning, & Renner, 2016). This photoperiod index, however, was not significantly correlated with latitude (Fig. 5f), suggesting that photoperiod alone cannot account for the spatial difference in temporal trends in the start of thermal and green season. The spatial variation of δSOS may be mainly driven by spatial differences in the rates of warming and by local environmental constraints on the start of green season.

δEOS was large at low latitudes and small at high latitudes (Fig. 4). The end of thermal season was consistently delayed across all latitudes, whereas the end of green season varied with latitude, with temporal advances at low latitudes and slight delays at high latitudes ($P < 0.01$) (Fig. S13c). These results may indicate a larger photoperiod limitation of the end of green season at higher latitudes, and we found that the standard deviation of the end of green season decreased with increasing latitude (-0.23 ± 0.12 d °N^{-1}, $P < 0.1$) (Fig. 5f), suggesting a larger effect of photoperiod at high latitudes. Water stress has mainly increased in central–southern Europe (Spinoni, Vogt, Naumann, Barbosa, & Dosio, 2018; Vicente-Serrano et al., 2014), which may also partially account for the temporal advance in the end of green season at lower latitudes. These

results indicate that spatial variation in δEOS can mainly be attributed to differences in local environmental constraints rather than to differences in the rates of autumnal warming.

Conclusion

This study found that global warming is extending both the thermal (potential) and the green (actual) season, as rated by flushing date and autumnal color change, of temperate deciduous trees, but trees are not exploiting the full window of opportunity of the potential green season. On average, trees' actual green season extensions lag behind extensions of the thermal potential by 7.9–11.1 days (65–86%) during the period 1980-2016. We further demonstrated that the increasing discrepancy between the lengths of the thermal and green seasons was mainly driven by the strong advances in the thermal onset of the thermal season that were not followed by proportionate advances in actual leaf-out dates. Our findings are consistent with previous reports showing that climate warming leads to a northward expansion of the cold range limits and productivity isolines of forests trees (Keenan et al., 2014; Lucht, Schaphoff, Erbrecht, Heyder, & Cramer, 2006; Richardson et al., 2010), but at a much slower pace relative to Northern Hemisphere-wide changes in temperature isolines (Huang et al., 2017). These results suggest that thermal acclimation needs to be accounted for in dynamic global vegetation models – which commonly rely on constant thermal requirements (Piao et al., 2014; Vickers et al., 2016) – to improve simulations of

vegetation distribution and ecosystem productivity. The mismatch between the responses of vegetation and the thermal growth potential is projected to increase as climatic warming continues (Mora et al., 2015). We therefore call for more efforts to explore the mechanisms underlying phenological shifts in response to the ongoing climate change, and call for caution when using thermal sums to predict future changes in plant vegetative growth or any processes involving plant development.

Materials and methods

Data set and definition. In-situ phenological data were obtained from the open-access Pan European Phenology Network (PEPN, http://www.pep725.eu/) and applied to carry out the main analysis (without specifically declaration of source of data). We selected totals of 1773 sites and six tree species with dates for both leaf-out (BBCH 11, first leaves unfolded) and foliar senescence (BBCH 94, 50% of leaves discoloured, which represents the percentage of discoloured leaves in the entire canopy, indicating that the canopy is undergoing a process of leaf senescence) for 1980-2016. We defined the actual vegetation-based green season (hereafter designated as GS) as the period between leaf-out (start of green season) and foliar senescence (end of green season). Climatic data were derived from a gridded climatic data set which fully considers the impact of topography and with a spatial resolution of 0.25° (Beer et al., 2014; Haylock et al., 2008; Van den Besselaar, Haylock, Van der Schrier, & Klein Tank, 2011), including daily mean air temperature, daily cumulative precipitation and daily shortwave radiation. We used meteorological data from the grid closest to an In-situ

phenological site to calculate the thermal start/end of growing season of that site. The start of thermal season was defined as the first day of the year when daily mean temperatures were >5 ℃ for more than five consecutive days, and the end of thermal season was defined as the day when daily mean temperatures were <5 ℃ for more than five days after 1 July, which is a simplify way that ignores the asymmetrical driving mechanism between spring and autumn phenology(Frich et al., 2002; Zhou, Zhai, Chen, & Yu, 2018). The thermal season length (TS) was determined as the interval between start and end of the thermal season. To further test the sensitivity of the TS estimation to the temperature thresholds, we estimated the TS and the difference between TS and GS (δGS) using temperature thresholds from 1℃ to 10 ℃ with one-degree step. We found similar results across temperature thresholds (Fig. S4), i.e. larger TS than GS, but interestingly the δGS was largest when we chose the 5℃ as the temperature threshold, which is precisely the threshold generally used in previous studies (Carter, 1998; Lallukka, Rantanen, & Mukula, 1978; Sarvas, 1972).

With the emergence and rapid development of remote sensing techniques, phenology observations are no longer limited to traditional in situ ground observation. To compare with the in situ-based species-level results, i.e. difference in GS and TS, at the community level (across species), remote sensing-based phenology data, i.e. vegetation-based start and end of season, with a spatial resolution of 0.25°, covering 1982-2015 were estimated using five different phenological extraction methods, which

include multiple fitting procedures to improving data quality and reduce uncertainty (i.e., the HANTS-Maximum method, Spline-Midpoint method, Gaussian-Midpoint method, Timesat-SG method, and Polyfit-Maximum method), that were used in previous studies with an extract threshold of 0.5 (Cong et al., 2012; Y. H. Fu et al., 2021), from the $GIMMS_{3g}$ NDVI data (https://climatedataguide.ucar.edu/climate-data/ndvi-normalized-difference-vegetation-index-3rd-generation-nasagfsc-gimms).

Spring warming model is a one-phase model that only consider the forcing process, which calculates the accumulated daily rats of forcing (R_f) applying a logistic function as below:

$$S_f = \sum_{t_0}^{t} R_f = \sum_{t_0}^{t} \frac{A_f}{1 + e^{\alpha (T - \beta)}}$$

Where S_f represents a daily sum of forcing rates, Af, α and β are the parameters take effect during forcing. The S_f begins to accumulate start from t_0, which is January 1st of current year.

The Sequential model is a two-phase model which assumes that the accumulation of forcing (S_f, a daily sum of forcing rates) starting after the chilling requirement (C_{crit}) is reached (Kramer, 1994). While another two-phase model (Parallel model) assumes that the accumulation of forcing functions when a critical threshold (C_{crit}) of chilling state (S_c, a daily sum of chilling rates) has not been attained (Landsberg, 1974). A triangular function and a logistic function with a competence function (K), note that the Parallel

model introduces another parameter (Kmin) which determining the minimum potential

of an unchilled bud to respond to the forcing temperature, were used to calculate the rate of chilling (R_c) and R_f, respectively. So, the state of chilling and forcing increasing simultaneously over time:

$$R_c = \begin{cases} 0, & T \le T_a \\ \dfrac{T - T_a}{T_b - T_a}, & T_a < T < T_b \\ \dfrac{T - T_c}{T_b - T_c}, & T_b < T < T_c \\ 0, & T \ge T_c \end{cases} \tag{3}$$

$$R_f = \begin{cases} 0, & T \le T_d \\ K \dfrac{Af}{1 + e^{\alpha (T + \beta)}}, & T > T_d \end{cases} \tag{4}$$

$$K_{Sequental} = \begin{cases} 0, & S_c < C_{crit} \\ 1, & S_c \ge C_{crit} \end{cases} \tag{5}$$

$$K_{Parallel} = \begin{cases} k_{min} + \dfrac{1 - k_{min}}{C_{crit}} S_c, & S_c < C_{crit} \\ 1, & S_c \ge C_{crit} \end{cases} \tag{5}$$

where $T_{a\text{-}d}$ are the parameters associated with chilling, and Af, α, β and K_{min} represent the parameters take effect during forcing. The S_c and S_f begins to accumulate after September 1 of the previous year.

We parameterized these models of each site through PSO (Particle swarm optimization) algorithm by setting the swarm number as 50, maximum number of iterations as 1000 and the expected value of the objective function (RMSE, root mean square error) as 1, based on the in situ SOS records before 1998, which splits 1980-2016 into two periods

of the same length (Marini & Walczak, 2015). And then, we applied three models to estimate the SOS of six species in each site during 1980-2016.

Statistical analysis.

Determination of the temporal trend of long time-series data and the latitudinal trend. We used a simple linear regression analysis to retrieve the long-term trend of variation in phenology (with year as the independent variable and phenological date as the dependent variable) and the spatial patterns of the main variables (e.g., δSOS, δEOS, δGS, temporal changes in chill days, seasonal precipitation, standard deviation of phenological dates) by setting latitude as the independent variable. We also used mixed-effects models (lmer function from the lme4 package in R) to determine if δGS was affected by δSOS and δEOS by taking species and sites into consider as random effects. Mixed-effects models were of the general form as:

$$y_{effect} = \beta_0 + \beta_1 x_{fixed} + b + \varepsilon$$

where y_{effect} is the effect size; β_0 is the intercept; β_1 is the coefficient associated with the fixed effect, x_{fixed}; b is the coefficient of the random effect (species and sites); and ε is the remaining variation.

Determination of optimal preseason. To exclude the covariate effects of other environmental factors, we obtained partial correlations between phenological dates and

average temperature during a specific period (ranging from 15 to 120 d, with steps of 15 d) before the mean phenological dates, using cumulative precipitation and shortwave

solar radiation as control variables. The optimal preseason was determined as the period for which average temperature had the largest absolute partial correlation coefficient with the phenological dates (R_T). We adopted the optimal preseason for specific sites and species in the subsequent analysis. The mean preseasons for the spring and autumnal (Although the main drivers that control autumn leaf senescence are photoperiod and autumn nighttime temperature, recent studies have found that summer climate involved the autumn leaf senescence processes (G. Liu et al., 2018; Zani et al., 2020)) vegetation phenologies across all species and sites were 53 ± 26 d (mean ± SD) and 64 ± 36 d, respectively (Fig. S14).

Apparent sensitivity to temperature (S_T) was defined as the advance (spring) or delay (autumn) of phenological date for every one degree increase in air temperature and was determined using reduced major-axis regression between the phenological dates and average air temperature during the optimal preseason.

Quantification of the relative contributions of spring and autumn phenology to the overall changes in growing season length. The relative contribution (CON) of spring and autumn phenology to the overall changes in green season length were calculated as(Garonna et al., 2014):

$$CON = (abs(Tr.SOS) - abs(Tr.EOS)) / (abs(Tr.SOS) + abs(Tr.EOS))$$

where Tr.SOS and Tr.EOS are the temporal trends of spring and autumn phenology, respectively, expressed in d decade^{-1}. A negative CON indicates that the changes in green season length were mostly attributed to the changes in autumn phenology, whereas a positive CON indicates that that the shift of spring phenology contributed more to the changes in green season length.

Chill days was defined as the number of days when temperature within a specific range (base temperature). In the present study, we counted the chilling days when daily mean temperature falls into the range between 0 and 5 ℃ following previous study (Y. H. Fu, Zhao, et al., 2015; H. Wang et al., 2020), and spanned from the previous 1st November to the average phenological date for spring leaf-out. Although the average daily mean temperature can fluctuate between -3 and +15 ℃ when the average daily mean temperature is between 0 and 5 ℃, some studies suggest that there is actually a much wider range of temperatures that chilling function (Baumgarten, Zohner, Gessler, & Vitasse, 2021). We used the same methodology to estimate the cold days for autumnal phenology and calculated the days from the summer solstice (21th June) to the average

date of foliar senescence (base temperature of 25 ℃)(Dufrêne et al., 2005) during 1980-2016 for each site.

Acknowledgements

The work was supported by the National Science Fund for Distinguished Young Scholars (42025101), the joint fund for regional innovation and development of NSFC (U21A2039), the Joint China-Sweden Mobility Program (Grant No. CH2020-8656), the 111 Project (B18006). JP acknowledges the financial support from the Spanish Government grant PID2019-110521GB-I00, the Fundación Ramón Areces grant ELEMENTAL-CLIMATE, and the Catalan Government grant SGR 2017-1005. The authors thank all members of the PEP725 project for providing the phenological data, and thank the two anonymous reviewers for their constructive suggestions and comments, which helped to improve the quality of the paper.

Author contributions

YHF conceived the ideas and designed methodology; XJG and SZC. analyzed the data and YHF led the writing of the manuscript in corporation with XZ, XJG and SZC; All authors contributed critically to the drafts and gave final approval for publication.

Competing interests

The authors declare no competing interests.

References

Asshoff, R., Zotz, G., & Körner, C. (2006). Growth and phenology of mature temperate forest trees in elevated CO2. Global Change Biology, 12(5), 848-861.

Augspurger, C. K. (2013). Reconstructing patterns of temperature, phenology, and frost damage over 124 years: spring damage risk is increasing. Ecology, 94(1), 41-50.

Baumgarten, F., Zohner, C. M., Gessler, A., & Vitasse, Y. (2021). Chilled to be forced: the best dose to wake up buds from winter dormancy. New Phytologist, 230(4), 1366-1377.

Beck, P. S., & Goetz, S. J. (2011). Satellite observations of high northern latitude vegetation productivity changes between 1982 and 2008: ecological variability and regional differences. Environmental Research Letters, 6(4), 045501.

Beer, C., Weber, U., Tomelleri, E., Carvalhais, N., Mahecha, M., & Reichstein, M. (2014). Harmonized European Long-Term Climate Data for Assessing the Effect of Changing Temporal Variability on Land–Atmosphere CO 2 Fluxes. Journal of Climate, 27(13), 4815-4834.

Carter, T. R. (1998). Changes in the thermal growing season in Nordic countries during the past century and prospects for the future. Agricultural and Food Science, 7(2), 161-179.

Chen, S., Fu, Y. H., Hao, F., Li, X., Zhou, S., Liu, C., & Tang, J. (2022). Vegetation phenology and its ecohydrological implications from individual to global scales. Geography and Sustainability.

Chmielewski, F.-M., & Rötzer, T. (2001). Response of tree phenology to climate change across Europe. Agricultural and Forest Meteorology, 108(2), 101-112.

Chuine, I. (2010). Why does phenology drive species distribution? Philosophical Transactions of the Royal Society B: Biological Sciences, 365(1555), 3149-3160.

Chuine, I., & Beaubien, E. G. (2001). Phenology is a major determinant of tree species range. Ecology Letters, 4(5), 500-510.

Chuine, I., Bonhomme, M., Legave, J. M., García de Cortázar–Atauri, I., Charrier, G., Lacointe, A., & Améglio, T. (2016). Can phenological models predict tree phenology accurately in the future? The unrevealed hurdle of endodormancy break. Global Change Biology, 22(10), 3444-3460.

Cleland, E. E., Chuine, I., Menzel, A., Mooney, H. A., & Schwartz, M. D. (2007). Shifting plant phenology in response to global change. Trends in Ecology & Evolution, 22(7), 357-365.

Cong, N., Piao, S., Chen, A., Wang, X., Lin, X., Chen, S., . . . Zhang, X. (2012). Spring vegetation green-up date in China inferred from SPOT NDVI data: A multiple model analysis. Agricultural and Forest Meteorology, 165, 104-113. doi:10.1016/j.agrformet.2012.06.009

Dufrêne, E., Davi, H., François, C., Le Maire, G., Le Dantec, V., & Granier, A. (2005). Modelling carbon and water cycles in a beech forest: Part I: Model description and uncertainty analysis on modelled NEE. Ecological Modelling,

185(2-4), 407-436.

Fang, J., & Lechowicz, M. J. (2006). Climatic limits for the present distribution of beech (Fagus L.) species in the world. Journal of Biogeography, 33(10), 1804-1819.

Frich, P., Alexander, L. V., Della-Marta, P., Gleason, B., Haylock, M., Tank, A. K., & Peterson, T. (2002). Observed coherent changes in climatic extremes during the second half of the twentieth century. Climate research, 19(3), 193-212.

Friend, A. D., Lucht, W., Rademacher, T. T., Keribin, R., Betts, R., Cadule, P., . . . Falloon, P. D. (2014). Carbon residence time dominates uncertainty in terrestrial vegetation responses to future climate and atmospheric CO2. Proceedings of the National Academy of Sciences, 111(9), 3280-3285.

Fu, Y. H., Geng, X., Hao, F., Vitasse, Y., Zohner, C. M., Zhang, X., . . . Piao, S. (2019). Shortened temperature‐relevant period of spring leaf‐out in temperate‐zone trees. Global Change Biology, 25(12), 4282-4290.

Fu, Y. H., Piao, S., Vitasse, Y., Zhao, H., De Boeck, H. J., Liu, Q., ... Janssens, I. A. (2015). Increased heat requirement for leaf flushing in temperate woody species over 1980–2012: effects of chilling, precipitation and insolation. Global Change Biology, 21(7), 2687-2697.

Fu, Y. H., Zhao, H., Piao, S., Peaucelle, M., Peng, S., Zhou, G., . . . Peñuelas, J. (2015). Declining global warming effects on the phenology of spring leaf unfolding. Nature, 526(7571), 104-107.

Fu, Y. H., Zhou, X., Li, X., Zhang, Y., Geng, X., Hao, F., . . . De Boeck, H. J. (2021). Decreasing control of precipitation on grassland spring phenology in temperate China. Global Ecology and Biogeography, 30(2), 490-499.

Fu, Y. S., Campioli, M., Vitasse, Y., De Boeck, H. J., Van den Berge, J., AbdElgawad, H., . . . Janssens, I. A. (2014). Variation in leaf flushing date influences autumnal senescence and next year’s flushing date in two temperate tree species. Proceedings of the National Academy of Sciences, 111(20), 7355-7360.

Garonna, I., De Jong, R., De Wit, A. J., Mücher, C. A., Schmid, B., & Schaepman, M. E. (2014). Strong contribution of autumn phenology to changes in satellite‐derived growing season length estimates across Europe (1982–2011). Global Change Biology, 20(11), 3457-3470.

Garonna, I., de Jong, R., & Schaepman, M. E. (2016). Variability and evolution of global land surface phenology over the past three decades (1982–2012). Global Change Biology, 22(4), 1456-1468.

Geng, X., Zhang, Y., Fu, Y. H., Hao, F., Janssens, I. A., Peñuelas, J., ...Zhang, J. (2022). Contrasting phenology responses to climate warming across the northern extra-tropics. Fundamental Research.

Haylock, M., Hofstra, N., Klein Tank, A., Klok, E., Jones, P., & New, M. (2008). A European daily high‐resolution gridded data set of surface temperature and precipitation for 1950–2006. Journal of Geophysical Research: Atmospheres, 113(D20).

Heberling, J. M., McDonough MacKenzie, C., Fridley, J. D., Kalisz, S., & Primack, R. B. (2019). Phenological mismatch with trees reduces wildflower carbon budgets.

Ecology Letters, 22(4), 616-623.

Hicke, J. A., Allen, C. D., Desai, A. R., Dietze, M. C., Hall, R. J., Hogg, E. H., . . . Sturrock, R. N. (2012). Effects of biotic disturbances on forest carbon cycling in the U nited S tates and C anada. Global Change Biology, 18(1), 7-34.

Hoffmann, A. A., & Sgrò, C. M. (2011). Climate change and evolutionary adaptation. Nature, 470(7335), 479-485.

Huang, M., Piao, S., Janssens, I. A., Zhu, Z., Wang, T., Wu, D., . . . Peng, S. (2017). Velocity of change in vegetation productivity over northern high latitudes. Nature Ecology & Evolution, 1(11), 1649-1654.

Jeong, S. (2020). Autumn greening in a warming climate. Nature Climate Change, 10(8), 712-713.

Keenan, T. F., Gray, J., Friedl, M. A., Toomey, M., Bohrer, G., Hollinger, D. Y., . . . Wing, I. S. (2014). Net carbon uptake has increased through warming-induced changes in temperate forest phenology. Nature Climate Change, 4(7), 598-604.

Keenan, T. F., & Richardson, A. D. (2015). The timing of autumn senescence is affected by the timing of spring phenology: implications for predictive models. Global Change Biology, 21(7), 2634-2641.

Kellermann, J. L., & van Riper, C. (2015). Detecting mismatches of bird migration stopover and tree phenology in response to changing climate. Oecologia, 178(4), 1227-1238.

Ketring, D., & Wheless, T. (1989). Thermal time requirements for phenological development of peanut. Agronomy Journal, 81(6), 910-917.

Kim, J. H., Hwang, T., Yang, Y., Schaaf, C. L., Boose, E., & Munger, J. W. (2018). Warming‐induced earlier greenup leads to reduced stream discharge in a temperate mixed forest catchment. Journal of Geophysical Research: Biogeosciences, 123(6), 1960-1975.

Körner, C., Basler, D., Hoch, G., Kollas, C., Lenz, A., Randin, C. F., . . . Zimmermann, N. E. (2016). Where, why and how? Explaining the low‐temperature range limits of temperate tree species. Journal of Ecology, 104(4), 1076- 1088.

Kramer, K. (1994). Selecting a model to predict the onset of growth of Fagus sylvatica. Journal of Applied Ecology, 172-181.

Lallukka, U., Rantanen, O., & Mukula, J. (1978). The temperature sum requirements of barley varieties in Finland. Paper presented at the Annales Agriculturae Fenniae.

Landsberg, J. (1974). Apple fruit bud development and growth; analysis and an empirical model. Annals of Botany, 38(5), 1013-1023.

Legg, S. (2021). IPCC, 2021: Climate Change 2021-the Physical Science basis. Interaction, 49(4), 44-45.

Li, X., Fu, Y. H., Chen, S., Xiao, J., Yin, G., Li, X., . . . Zhou, X. (2021). Increasing importance of precipitation in spring phenology with decreasing latitudes in subtropical forest area in China. Agricultural and Forest Meteorology, 304, 108427.

Linderholm, H. W. (2006). Growing season changes in the last century. Agricultural and Forest Meteorology, 137(1-2), 1-14.

Liu, G., Chen, X., Zhang, Q., Lang, W., & Delpierre, N. (2018). Antagonistic effects of growing season and autumn temperatures on the timing of leaf coloration in winter deciduous trees. Global Change Biology, 24(8), 3537-3545.

Liu, Q., Piao, S., Janssens, I. A., Fu, Y., Peng, S., Lian, X., . . . Wang, T. (2018). Extension of the growing season increases vegetation exposure to frost. Nature communications, 9(1), 1-8.

Lucht, W., Schaphoff, S., Erbrecht, T., Heyder, U., & Cramer, W. (2006). Terrestrial vegetation redistribution and carbon balance under climate change. Carbon balance and management, 1(1), 1-7.

Maino, J. L., Kong, J. D., Hoffmann, A. A., Barton, M. G., & Kearney, M. R. (2016). Mechanistic models for predicting insect responses to climate change. Current opinion in insect science, 17, 81-86.

Marini, F., & Walczak, B. (2015). Particle swarm optimization (PSO). A tutorial. Chemometrics and Intelligent Laboratory Systems, 149, 153-165.

Menzel, A., Yuan, Y., Matiu, M., Sparks, T., Scheifinger, H., Gehrig, R., & Estrella, N. (2020). Climate change fingerprints in recent European plant phenology. Global Change Biology, 26(4), 2599-2612.

Mora, C., Caldwell, I. R., Caldwell, J. M., Fisher, M. R., Genco, B. M., & Running, S. W. (2015). Suitable days for plant growth disappear under projected climate change: Potential human and biotic vulnerability. PLoS Biology, 13(6), e1002167.

Park, T., Ganguly, S., Tømmervik, H., Euskirchen, E. S., Høgda, K.-A., Karlsen, S. R., . . . Myneni, R. B. (2016). Changes in growing season duration and productivity of northern vegetation inferred from long-term remote sensing data. Environmental Research Letters, 11(8), 084001.

Peaucelle, M., Janssens, I. A., Stocker, B. D., Descals Ferrando, A., Fu, Y. H., Molowny-Horas, R., . . . Peñuelas, J. (2019). Spatial variance of spring phenology in temperate deciduous forests is constrained by background climatic conditions. Nature Communications, 10(1), 1-10.

Peñuelas, J., Rutishauser, T., & Filella, I. (2009). Phenology feedbacks on climate change. Science, 324(5929), 887-888.

Piao, S., Liu, Q., Chen, A., Janssens, I. A., Fu, Y., Dai, J., . . . Zhu, X. (2019). Plant phenology and global climate change: Current progresses and challenges. Global Change Biology, 25(6), 1922-1940.

Piao, S., Nan, H., Huntingford, C., Ciais, P., Friedlingstein, P., Sitch, S., . . . Cong, N. (2014). Evidence for a weakening relationship between interannual temperature variability and northern vegetation activity. Nature communications, 5(1), 1-7.

Piao, S., Wang, X., Park, T., Chen, C., Lian, X., He, Y., . . . Tømmervik, H. (2020). Characteristics, drivers and feedbacks of global greening. Nature Reviews Earth & Environment, 1(1), 14-27.

Prevéy, J., Vellend, M., Rüger, N., Hollister, R. D., Bjorkman, A. D., Myers-Smith,

I. H., . . . Elberling, B. (2017). Greater temperature sensitivity of plant phenology at colder sites: implications for convergence across northern latitudes. Global Change Biology, 23(7), 2660-2671.

Renner, S. S., & Zohner, C. M. (2018). Climate change and phenological mismatch in trophic interactions among plants, insects, and vertebrates. Annual Review of Ecology, Evolution, and Systematics, 49, 165-182.

Richardson, A. D., Andy Black, T., Ciais, P., Delbart, N., Friedl, M. A., Gobron, N., . . . Luyssaert, S. (2010). Influence of spring and autumn phenological transitions on forest ecosystem productivity. Philosophical Transactions of the Royal Society B: Biological Sciences, 365(1555), 3227-3246.

Sarvas, R. (1972). Investigations on the annual cycle of development of forest trees. Active period. Investigations on the annual cycle of development of forest trees. Active period., 76(3).

Scherrer, D., Vitasse, Y., Guisan, A., Wohlgemuth, T., & Lischke, H. (2020). Competition and demography rather than dispersal limitation slow down upward shifts of trees' upper elevation limits in the Alps. Journal of Ecology, 108(6), 2416-2430.

Spinoni, J., Vogt, J. V., Naumann, G., Barbosa, P., & Dosio, A. (2018). Will drought events become more frequent and severe in Europe? International Journal of Climatology, 38(4), 1718-1736.

Tang, J., Körner, C., Muraoka, H., Piao, S., Shen, M., Thackeray, S. J., & Yang, X. (2016). Emerging opportunities and challenges in phenology: a review. Ecosphere, 7(8), e01436.

Trumbore, S., Brando, P., & Hartmann, H. (2015). Forest health and global change. Science, 349(6250), 814-818.

Van den Besselaar, E. J., Haylock, M., Van der Schrier, G., & Klein Tank, A. (2011). A European daily high‐resolution observational gridded data set of sea level pressure. Journal of Geophysical Research: Atmospheres, 116(D11).

Vicente-Serrano, S. M., Lopez-Moreno, J.-I., Beguería, S., Lorenzo-Lacruz, J., Sanchez-Lorenzo, A., García-Ruiz, J. M., . . . Trigo, R. (2014). Evidence of increasing drought severity caused by temperature rise in southern Europe. Environmental Research Letters, 9(4), 044001.

Vickers, H., Høgda, K. A., Solbø, S., Karlsen, S. R., Tømmervik, H., Aanes, R., & Hansen, B. B. (2016). Changes in greening in the high Arctic: insights from a 30 year AVHRR max NDVI dataset for Svalbard. Environmental Research Letters, 11(10), 105004.

Vitasse, Y., Bottero, A., Cailleret, M., Bigler, C., Fonti, P., Gessler, A., . . . Rigling, A. (2019). Contrasting resistance and resilience to extreme drought and late spring frost in five major European tree species. Global Change Biology, 25(11), 3781-3792.

Vitasse, Y., Ursenbacher, S., Klein, G., Bohnenstengel, T., Chittaro, Y., Delestrade, A., . . . Strebel, N. (2021). Phenological and elevational shifts of plants, animals and fungi under climate change in the E uropean A lps. Biological Reviews, 96(5), 1816-1835.

Wang, H., Wu, C., Ciais, P., Penuelas, J., Dai, J., Fu, Y., & Ge, Q. (2020). Overestimation of the effect of climatic warming on spring phenology due to misrepresentation of chilling. Nature Communications, 11(1), 1-9.

Wang, J., Liu, D., Ciais, P., & Peñuelas, J. (2022). Decreasing rainfall frequency contributes to earlier leaf onset in northern ecosystems. Nature Climate Change, 1-7.

Wu, D., Zhao, X., Liang, S., Zhou, T., Huang, K., Tang, B., & Zhao, W. (2015). Time-lag effects of global vegetation responses to climate change. Global Change Biology, 21(9), 3520-3531.

Zani, D., Crowther, T. W., Mo, L., Renner, S. S., & Zohner, C. M. (2020). Increased growing-season productivity drives earlier autumn leaf senescence in temperate trees. Science, 370(6520), 1066-1071.

Zhang, J., Xiao, J., Tong, X., Zhang, J., Meng, P., Li, J., . . . Yu, P. (2022). NIRv and SIF better estimate phenology than NDVI and EVI: Effects of spring and autumn phenology on ecosystem production of planted forests. Agricultural and Forest Meteorology, 315, 108819.

Zhou, B., Zhai, P., Chen, Y., & Yu, R. (2018). Projected changes of thermal growing season over Northern Eurasia in a 1.5 C and 2 C warming world. Environmental Research Letters, 13(3), 035004.

Zhu, W., Tian, H., Xu, X., Pan, Y., Chen, G., & Lin, W. (2012). Extension of the growing season due to delayed autumn over mid and high latitudes in North America during 1982-2006. Global Ecology and Biogeography, 21(2), 260-271.

Zimmermann, A., Webber, H., Zhao, G., Ewert, F., Kros, J., Wolf, J., . . . de Vries, W. (2017). Climate change impacts on crop yields, land use and environment in response to crop sowing dates and thermal time requirements. Agricultural Systems, 157, 81-92.

Zohner, C. M., Benito, B. M., Svenning, J.-C., & Renner, S. S. (2016). Day length unlikely to constrain climate-driven shifts in leaf-out times of northern woody plants. Nature Climate Change, 6(12), 1120-1123.

Figure legends

Figure 1. Changes in the temporal trends of the thermal season length (TS) and actual green season (GS) during 1980-2016. (a) Frequency distributions of the temporal trend of GS, TS and the difference between them (δGS) across all sites and species. The dashed line denotes no trend. (b) The distributions and relationship between GS and TS. The subpanels show the frequency and distribution of significance of the data in each quadrant. (c) Changes in the temporal trend of the length of the green season for each species. The data in the boxes represent averages and the fraction of the data with significant temporal trends. AH, *Aesculus hippocastanum* (horse chestnut); BP, *Betula pendula* (silver birch); BPu, *Betula pubescens* (white birch); FS, *Fagus sylvatica* (beech); QR, *Quercus robur* (oak); TC, *Tilia cordata* (lime). The number of sites for each species are in brackets below the species name.

Figure 2. Changes in the temporal trends of the thermal season length (TS) and remote sensing-based green season (GS) during 1982-2015. (a) Spatial pattern of δGS (the difference between TS and GS) Trend. (b) Frequency distributions of the temporal trend of GS, TS and the difference between them (δGS) in study area. The dashed line denotes no trend.

Figure 3. Changes in the temporal trends of the start (SOS) and end (EOS) of the growing season during 1980-2016. (a) Frequency distributions of the temporal trends of the start of the vegetative growing season (VSOS), start of the thermal growing

season (TSOS) and the difference between them (δSOS) for all sites and species. (b) Frequency distributions of the temporal trends of the end of the vegetative growing season (VEOS), end of the thermal growing season (TEOS) and the difference between them (δEOS). The dashed lines in (a) and (b) denote no trends. (c) Temporal trends of the start and end of the growing season for each species. AH, *Aesculus hippocastanum* (horse chestnut); BP, *Betula pendula* (silver birch); BPu, *Betula pubescens* (white birch); FS, *Fagus sylvatica* (beech); QR, *Quercus robur* (oak); TC, *Tilia cordata* (lime).

Figure 4. Spatial variability of the temporal trends in δGS, δSOS and δEOS with latitude. (a) Changes in the temporal trend of the difference between the canopy duration of temperate trees and thermal growing season length (δGS) with latitude. (b) Changes in the temporal trend of the difference between the start and end of the vegetation-based and thermal growing seasons (δSOS and δEOS) with latitude. All data were averaged every 0.25° northward. δSOS was the opposite of the original data. The shading represents the 95% confidence intervals. The subpanels show the proportion of positive and negative values of the site and species data and their significance.

Figure 5. Possible effects of environmental variables. (a) Temporal trend of seasonal temperature in spring (MAM; March, April and May), summer (JJA; June, July and August), autumn (SON; September, October and November) and winter (DJF; December, January and February). The subpanel shows the average and standard deviation of the seasonal warming trends. (b) Frequency distribution of the correlation

coefficient between phenological date and temperature determined using a partial correlation analysis that excluded the influence of precipitation and shortwave radiation. The subpanel shows the proportion of positive and negative values and the significance. (c) Apparent sensitivities to temperature for the start and end of the vegetation-based growing season (VSOS and VEOS, respectively). The central marks indicate the medians, and the bottom and top edges of the boxes indicate the 25th and 75th percentiles, respectively. The subpanel shows the frequency distribution of the sensitivities to temperature. (d) Distribution of the temporal changes in chill days for VSOS and VEOS. The subpanel shows the spatial pattern of temporal changes in chill days. The values in brackets indicate the slope and significance (*P* value) of the linear fitting. (e) Spatial pattern of temporal changes in seasonal precipitation. (f) Variation of the deviation of phenological dates with latitude. The data for (e), (f) and the subpanel in (d) are averaged every 0.25° northward. The shading represents the 95% confidence intervals.

Fig. 1

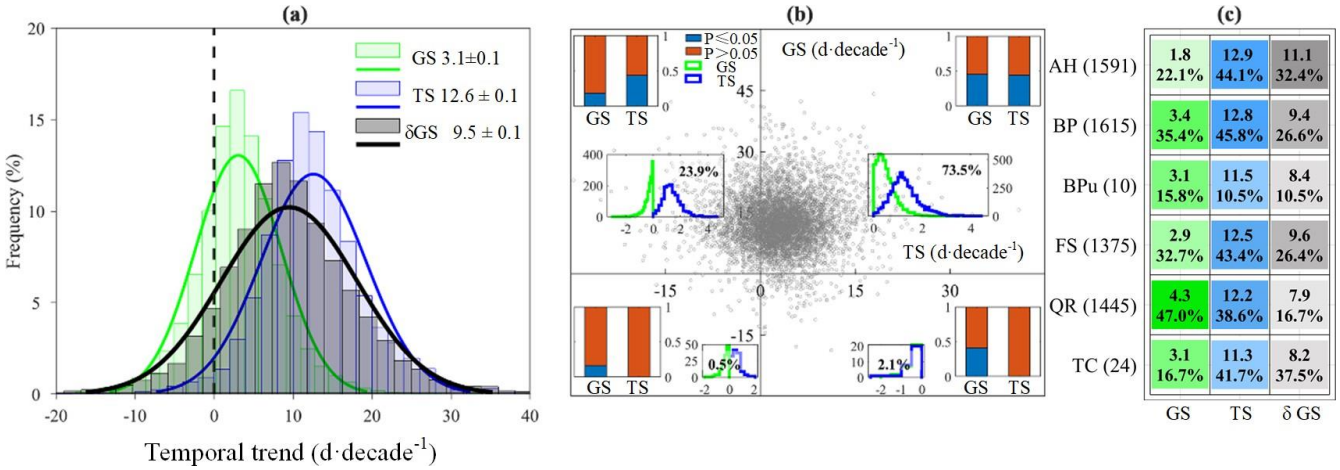
(a)
GS 3.1±0.1
TS 12.6 ± 0.1
δGS 9.5 ± 0.1
Frequency (%)
Temporal trend (d·decade-1)
(b)
P≤0.05
P>0.05
GS
TS
GS (d·decade-1)
TS (d·decade-1)
23.9%
73.5%
0.5%
2.1%
(c)
AH (1591)
BP (1615)
BPu (10)
FS (1375)
QR (1445)
TC (24)
GS
TS
δ GS
1.8 22.1%
12.9 44.1%
11.1 32.4%
3.4 35.4%
12.8 45.8%
9.4 26.6%
3.1 15.8%
11.5 10.5%
8.4 10.5%
2.9 32.7%
12.5 43.4%
9.6 26.4%
4.3 47.0%
12.2 38.6%
7.9 16.7%
3.1 16.7%
11.3 41.7%
8.2 37.5%

Fig. 2

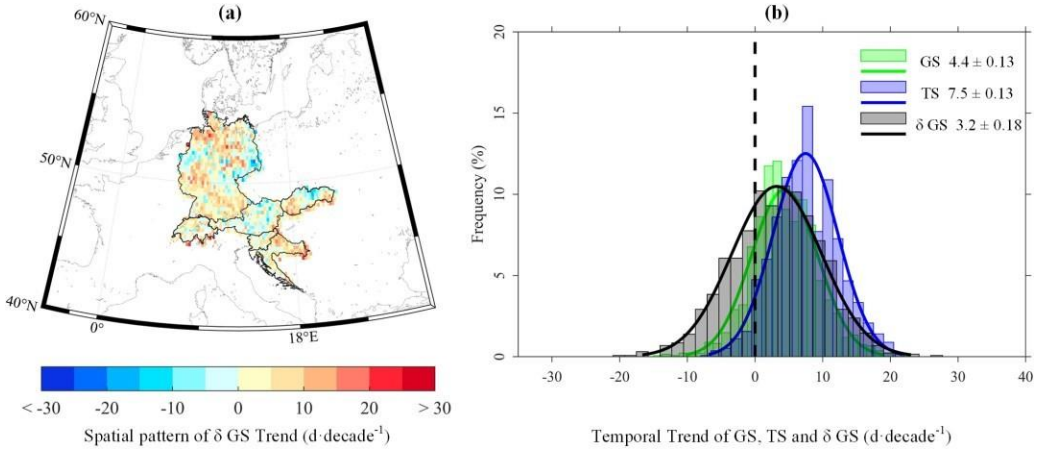
(a)
60°N
50°N
40°N
0°
18°E
< -30
-20
-10
0
10
20
> 30
Spatial pattern of δ GS Trend (d·decade-1)
(b)
GS 4.4 ± 0.13
TS 7.5 ± 0.13
δ GS 3.2 ± 0.18
Frequency (%)
Temporal Trend of GS, TS and δ GS (d·decade-1)

Fig. 3

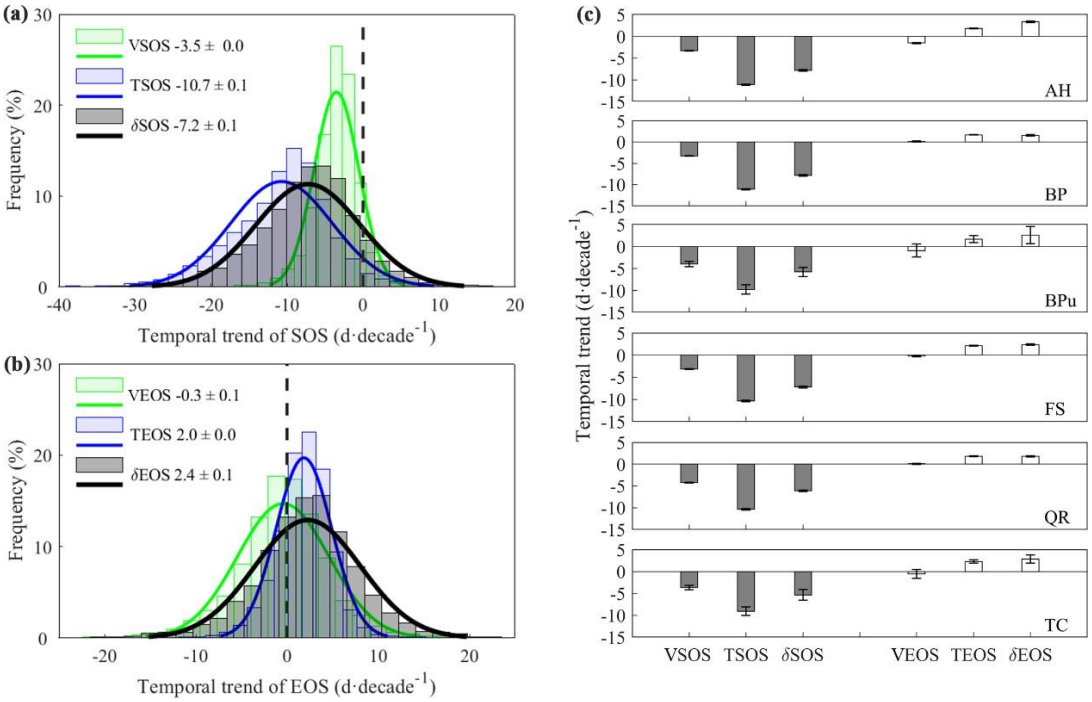
(a)
VSOS -3.5 ± 0.0
TSOS -10.7 ± 0.1
δSOS -7.2 ± 0.1
Frequency (%)
Temporal trend of SOS (d·decade-1)
(b)
VEOS -0.3 ± 0.1
TEOS 2.0 ± 0.0
δEOS 2.4 ± 0.1
Frequency (%)
Temporal trend of EOS (d·decade-1)
(c)
Temporal trend (d·decade-1)
AH
BP
BPu
FS
QR
TC
VSOS TSOS δSOS VEOS TEOS δEOS

Fig. 4

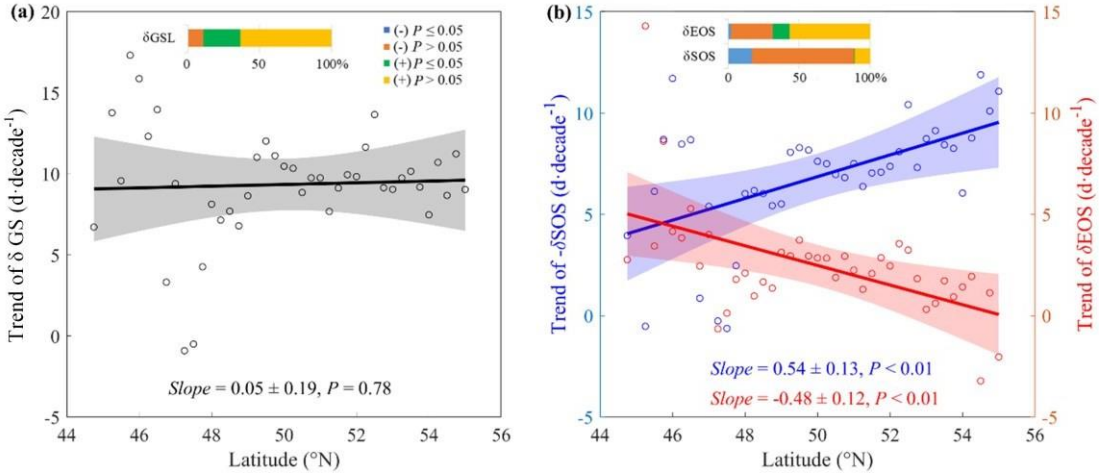
(a)
δGSL
0
50
100%
(-) P ≤ 0.05
(-) P > 0.05
(+) P ≤ 0.05
(+) P > 0.05
Trend of δ GS (d·decade-1)
Slope = 0.05 ± 0.19, P = 0.78
Latitude (°N)
(b)
δEOS
δSOS
Trend of -δSOS (d·decade-1)
Trend of δEOS (d·decade-1)
Slope = 0.54 ± 0.13, P < 0.01
Slope = -0.48 ± 0.12, P < 0.01
Latitude (°N)

Fig. 5

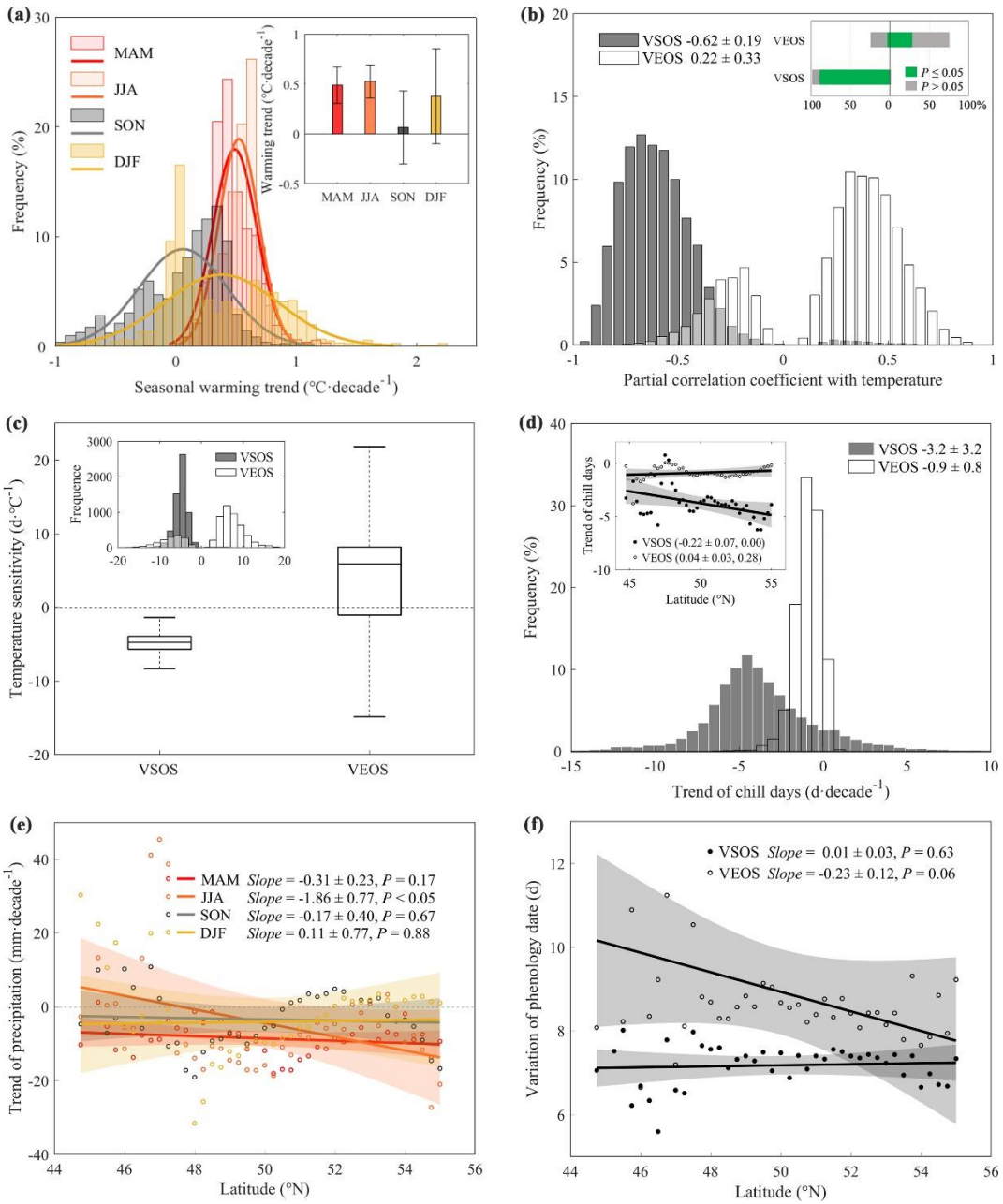
(a)
MAM
JJA
SON
DJF
Frequency (%)
Seasonal warming trend (°C·decade^{-1})
Warming trend (°C·decade^{-1})
MAM JJA SON DJF
(b)
VSOS -0.62 ± 0.19
VEOS 0.22 ± 0.33
VEOS
VSOS
P ≤ 0.05
P > 0.05
Frequency (%)
Partial correlation coefficient with temperature
(c)
VSOS
VEOS
Frequence
Temperature sensitivity (d·°C^{-1})
VSOS
VEOS
(d)
VSOS -3.2 ± 3.2
VEOS -0.9 ± 0.8
Trend of chill days
VSOS (-0.22 ± 0.07, 0.00)
VEOS (0.04 ± 0.03, 0.28)
Latitude (°N)
Frequency (%)
Trend of chill days (d·decade^{-1})
(e)
MAM Slope = -0.31 ± 0.23, P = 0.17
JJA Slope = -1.86 ± 0.77, P < 0.05
SON Slope = -0.17 ± 0.40, P = 0.67
DJF Slope = 0.11 ± 0.77, P = 0.88
Trend of precipitation (mm·decade^{-1})
Latitude (°N)
(f)
VSOS Slope = 0.01 ± 0.03, P = 0.63
VEOS Slope = -0.23 ± 0.12, P = 0.06
Variation of phenology date (d)
Latitude (°N)